Evaluating Surface Energy Balance System (SEBS) using Aircraft data collected during BEAREX07

George Paul[1], Prasanna H. Gowda[2], P.V. Vara Prasad[3], Terry A. Howell[4], Scott A. Staggenborg[5]

[1]Graduate Research Assistant, Department of Agronomy, Kansas State University, Manhattan, KS 66506; Ph (785)532-7802; Fax (785)532-6094; email: gpaul@ksu.edu

[2]Agricultural Engineer, USDA-ARS Conservation and Production Research Laboratory, P.O. Drawer 10, Bushland, TX 79012; Ph (806)356-5730; Fax (806)356-5750; email: Prasanna.Gowda@ars.usda.gov

[3]Associate Professor, Department of Agronomy, Kansas State University, Manhattan, KS 66506; Ph (785)532-3746; Fax (785)532-6094; email: vara@ksu.edu

[4]Agricultural Engineer & Research Leader, USDA-ARS Conservation and Production Research Laboratory, P.O. Drawer 10, Bushland, TX 79012; Ph (806)356-5746; Fax (806)356-5750; email: Terry.Howell@ars.usda.gov

[5]Professor, Department of Agronomy, Kansas State University, Manhattan, KS 66506; Ph (785)532-7214; Fax (785)532-6094; email: sstaggen@ksu.edu

Abstract

Evapotranspiration (ET) is an essential component of the water balance and a major consumptive use of irrigation water and precipitation on cropland. Remote sensing based surface energy balance algorithms are now capable of providing accurate estimates of spatial-temporal ET. Uses of these spatial ET estimates are innumerable including hydrological modeling, irrigation scheduling, drought and flood monitoring and global climate change studies. The objective of this study was to evaluate the ability of the Surface Energy Balance System (SEBS) to estimate hourly ET fluxes using very high resolution (0.5-1.8 m) aircraft images acquired during the BEAREX07 (Bushland ET and Agricultural Remote Sensing Experiment 2007). Accuracy of the predicted ET fluxes were investigated using observed data from 4 large weighing lysimeters, each located at the center of 4.7 ha field in the USDA-ARS Conservation and Production Research Laboratory, Bushland, Texas. The uniqueness and the strength of this study come from the fact that it evaluates the SEBS for irrigated and dryland conditions simultaneously with each lysimeter field planted to irrigated forage sorghum, irrigated forage corn, dryland clumped-grain sorghum, and dryland row-grain sorghum. Eleven images acquired during early and mid cropping seasons (June 24 - July 27) were used in the study. SEBS algorithm performed equally well for both irrigated and dryland conditions in estimating the hourly ET with overall mean bias error and root mean square of -0.01 and 0.11 mm h^{-1} (-1.53% and 20.27%), respectively.

Introduction

Over the past three decades, numerous remote sensing based evapotranspiration (ET) algorithms have been developed. These algorithms provided a robust, economical, and efficient tool for estimating and mapping ET at field and regional scales. Accurate estimation of spatial ET has large utility including crop

water management, climate change impact assessment, hydrological modeling, recharge prediction, irrigation performance and land use planning. A detailed review of different remote sensing based ET algorithms is presented in Gowda et al. (2008). They reported that ET estimation accuracy varied from 67 to 97% for daily ET and above 94% for seasonal ET, indicating that remote sensing technology with appropriate algorithms has the potential to estimate ET adequately. However, operational utilization of these algorithms has not yet been taken up due to various limitations and requirements for more stringent evaluation under varying landscapes and agrometeorological conditions.

Surface Energy Balance System (SEBS) was developed by Su (2002) for the estimation of atmospheric turbulent fluxes using satellite earth observation data. SEBS adopts the concept from the SEBI (Surface Energy Balance Index) scheme (Menenti and Choudhury 1993). A better parameterization of turbulent heat transfer, and bulk atmospheric similarity theory has been integrated in SEBS (Menenti et al., 2003).

The aerodynamic resistance in a single source model is usually estimated on the basis of surface layer similarity theory. In single source models the radiometric surface temperature, measured by the remote sensing thermal sensors is assumed to be equivalent to the aerodynamic surface temperature. This approximation can be applied to heterogeneous land surfaces by adding an excess resistance term (kB^{-1}) to the aerodynamic resistance (Jia et al., 2003). SEBS provides a new parameterization of aerodynamic resistance to heat transfer (in terms of kB^{-1}) thus accounting for both aerodynamic excess resistance and radiometric excess resistance to relate sensible heat (H) to radiometric surface temperature.

SEBS was found to be sensitive to meteorological parameters (air temperature, air pressure and wind speed) and surface temperature in a study involving ASTER image and flux tower measurements (van der Kwast et al., 2009). Results of ET estimates, derived for multiple sensors (ETM, ASTER, MODIS) using SEBS were compared against eddy covariance flux tower measurements; reported difficulty in evaluating large scale remote sensing results over heterogeneous terrain (McCabe and Wood 2006). However, the SEBS has never been evaluated for its ability to estimate hourly ET fluxes from very high resolution remote sensing data in the semi-arid, highly advective, Texas High Plains. Therefore, the main objective of this study was to evaluate the Surface Energy Balance System (SEBS) to estimate hourly ET fluxes using very high resolution images in the Texas High Plains. Remote sensing data acquired during the Bushland Evapotranspiration and Agricultural Remote Sensing Experiment 2007 (BEAREX07) will be used for this purpose. An important aspect of the present study was that the SEBS algorithm was evaluated against the ET rates measured using four large weighing lysimeters, each located at the center of 4.7 ha field. The uniqueness and the strength of this study come from the fact that it evaluates SEBS algorithms for irrigated and dryland conditions simultaneously.

Materials and Methods

Study area and data acquisition

The BEAREX07 was conducted at the USDA-ARS Conservation and Production Research Laboratory (CPRL; Figure 1) during the 2007 summer cropping

season to enhance understanding of land surface hydro-meteorological process in the semi-arid, highly advective, Texas High Plains and to develop a comprehensive dataset for rigorous testing of remote sensing based ET models.

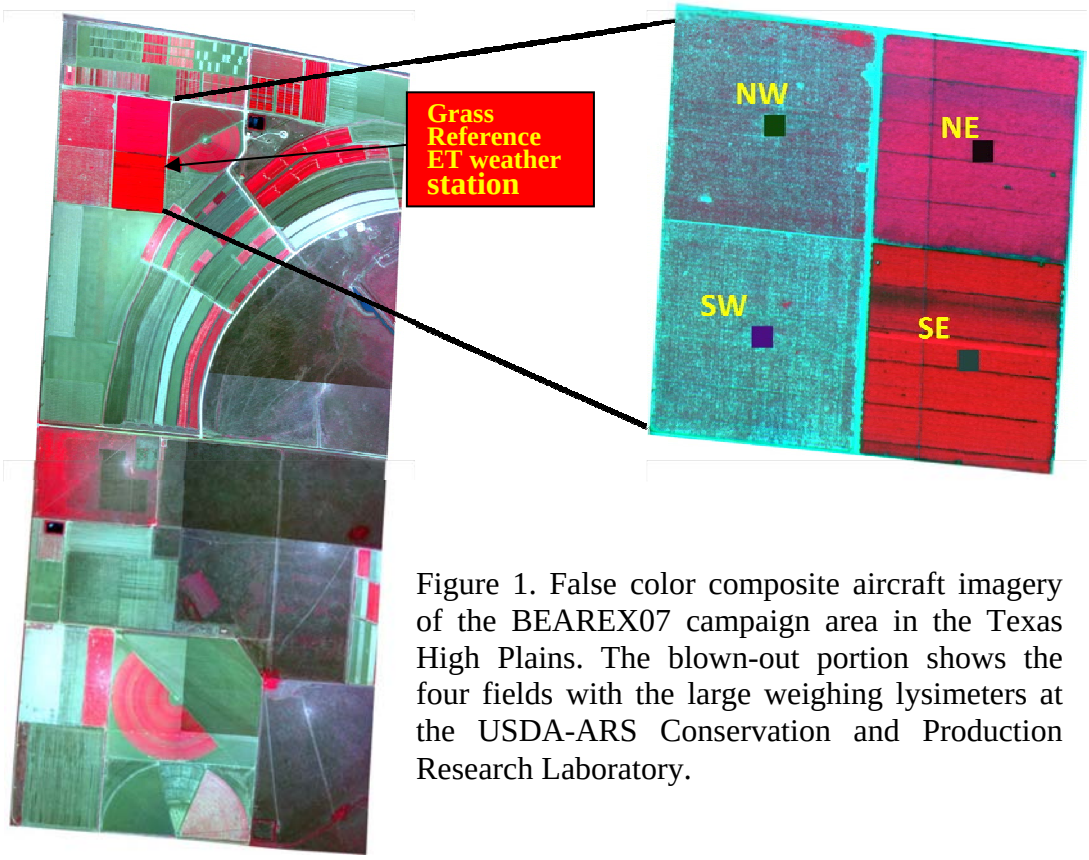

Figure 1. False color composite aircraft imagery of the BEAREX07 campaign area in the Texas High Plains. The blown-out portion shows the four fields with the large weighing lysimeters at the USDA-ARS Conservation and Production Research Laboratory.

The CPRL is the home of four large weighing lysimeters (3 m long, 3 m wide x 2.4 m deep) each located in the middle of a 4.7 ha fields arranged in a block pattern. Two lysimeters fields located on the east (NE and SE) are managed under irrigation management and two lysimeters on the west (NW and SW) are managed under dryland conditions. In 2007, the NE field was planted to forage sorghum (planted on May 30), the SE field was planted to forage corn (planted on May 17), the NW field was planted to grain sorghum in rows (planted on June 6), while the SW field was planted to grain sorghum (planted on June 6) in clumps. Each lysimeter field was equipped with net radiometer, infra-red thermometer, soil heat flux plates and for measuring net radiation, radiometric surface temperature, and soil heat fluxes, respectively. In addition a grass reference ET weather station field (0.31 ha), which is a part of the Texas High Plains ET Network (TXHPET, 2006) is located on the eastern edge of the irrigated lysimeter fields (Figure 1).

Flying expeditions were carried out to collect remotely sensed imagery using the Utah State University (USU) airborne digital multispectral system. The system acquired high resolution imagery in the visible, near infrared and thermal infrared portions of the electromagnetic spectrum. Visible and near infrared images were acquired at 0.5 m spatial resolution while the thermal images were acquired at 1.8 m. Eleven images acquired during the early cropping season (June 24 - July27) were

used to evaluate the SEBS algorithm in a GIS environment. Multiple images acquired during single day were included in the analysis to evaluate the capability of the algorithm in capturing the variations of energy fluxes and resistance terms. Image acquisition date and time with various weather parameter at the time of image acquisition are presented in Table 1.

Table 1: Image Acquisition date and various weather parameters

Date	Time (CST)	Julian Day	SW_in (Wm^{-2})	T_air (°C)	RH (%)	BP (kPa)	W. Speed (ms^{-1})
06/24/07	10:20	175	767.5	27.8	45	88.4	2.2
06/25/07	11:33	176	896.9	27.9	51	88.6	4.9
07/02/07	3:27	183	788.8	25.7	51	88.8	2.6
07/10/07	9:53	191	653.1	29.3	37	88.5	1.4
07/10/07	11:15	191	793.6	31.8	29	88.6	2.5
07/10/07	2:50	191	883.0	33.6	26	88.6	4.0
07/11/07	12:40	192	935.2	27.6	54	88.6	4.5
07/26/07	11:37	207	900.6	28.6	43	88.6	4.8
07/27/07	9:55	208	646.3	25.3	57	88.7	2.4
07/27/07	11:16	208	798.8	29.7	37	88.6	2.0
07/27/07	1:33	208	879.1	31.4	30	88.5	2.8

Surface Energy Balance System (SEBS)

Surface Energy Balance System (SEBS) is a single source land surface energy balance algorithm with a dynamic model for the thermal roughness, the Bulk Atmospheric Similarity theory for PBL scaling and the Monin-Obukhov Atmospheric Surface Layer (ASL) similarity for surface layer scaling. SEBS uses an excess resistance term that accounts for the fact that the roughness lengths for heat and momentum are different for canopy and soil surfaces. Primarily, three input data sets were utilized for executing the SEBS in this study: (1) albedo, emissivity, surface temperature and Normalized Difference Vegetation Index (NDVI) derived from remote sensing data (2) air pressure, air temperature, relative humidity, and wind speed measurements from weather stations, and (3) downward solar radiation.

Surface energy balance governs the water exchange and partition of the surface turbulent fluxes into sensible and latent heat in the soil-vegetation-atmosphere continuum. The residual method of surface energy balance is one of the most widely applied approaches to mapping ET at different temporal and spatial scales. In its simplest form the surface energy balance equation can be written as:

$$R_n = G_0 + H + LE \tag{7}$$

where, R_n is the net radiation, G_o is the soil heat flux, H is the sensible heat flux, and LE is the latent heat flux (L is the latent heat of vaporization and E is the actual evapotranspiration).

Net radiation (R_n) is the dominant term in the energy balance equation as it represents the source of energy that must be balanced by the thermodynamic

equilibrium of the other terms. The net radiation can also be expressed as an electromagnetic balance of all incoming and outgoing fluxes reaching and leaving a flat horizontal and homogeneous surface as:

$$R_n = (1-\alpha_o)S\downarrow + \varepsilon_a \sigma T_a^4 - \varepsilon_o \sigma T_s^4 \quad (8)$$

where α_o is the broadband surface albedo, $S\downarrow$ is the incoming shortwave radiation, ε_a is the emissivity of air, T_a is the air temperature, ε_o is the surface emissivity, T_s is the surface temperature and σ is Stefan-Bolzmann constant.

SEBS requires accurate values of land surface albedo and land surface temperature (Jia 2003). The broadband albedo was calculated as the total sum of the different in-band planetary albedos according to different weights for different bands. The bandpass solar exoatmospheric irradiance ($ESUN_\lambda$) is an average solar irradiance weighted by corresponding spectral band response function. It is computed from:

$$ESUN_\lambda = \frac{\sum\{E_o(\lambda)\times S(\lambda)\}\times\Delta\lambda}{\sum\{S(\lambda)\}\times\Delta\lambda} \quad (9)$$

where, $S(\lambda)$ is the wavelength dependent radiance spectral response also known as spectral response function for the sensor in $Wm^{-2}\mu m^{-1}$, $E_o(\lambda)$ is the top of the atmosphere solar irradiance or the extraterrestrial solar irradiance in $Wm^{-2}\mu m^{-1}$. The integration interval is within the pass band of the sensor; $\Delta\lambda$ is the wavelength interval taken as 0.005μm.

Table 2: Spectral band of the sensor with their respective weights

BAND	Wavelength (μm)	$ESUN_\lambda$ ($Wm^{-2}\mu m^{-1}$)	Weight
Green	0.545-0.560	1154.79	0.303609
Red	0.665-0.680	1521.50	0.400022
NIR	0.795-0.809	1127.25	0.296369

The weight for each band was calculated from equation 9 and is presented in Table 2. The equation for broadband albedo (α_o) can be written as:

$$\alpha_o = 0.303\times green + 0.400\times red + 0.296\times NIR \quad (10)$$

where green, red and NIR are the reflectance of the respective bands.

The remote sensing based variables that best explain the soil heat transport behavior are albedo, surface temperature and land cover vegetation index. The evaluation of G_o, usually presented as a ratio G_o/R_n, was adopted from Bastiaanssen et al (1998).

$$\frac{G_o}{R_n} = \frac{(T_s - 273.15)}{100\alpha_o}\left(0.32\alpha_o + 0.62\alpha_o^2\right)\left(1 - 0.98NDVI^4\right) \quad (11)$$

The apparent emissivity of the atmosphere is usually estimated with equations based on vapor pressure and temperature at the standard meteorological stations. For clear skies, the Brutsaert (1975) formulation was used as:

$$\varepsilon_a = 1.24\left(\frac{e_d}{T_a}\right)^{1/7} \quad (12)$$

where Ta is the air temperature [K], e_d is the vapor pressure [mbar]

In SEBS, the sensible heat flux (H) is estimated considering energy balance at limiting cases. Under dry-limit, the latent heat (LE_{dry}) becomes zero due to the limitation of soil moisture and the sensible heat flux (H_{dry}) is at maximum value (eq. 13 and 14).

$$LE_{dry} = R_n - G_0 - H_{dry} \equiv 0 \tag{13}$$

$$H_{dry} = R_n - G_0 \tag{14}$$

Under wet limit evaporation takes place at potential rate (LE_{wet}) and the sensible heat flux (H_{wet}) value is at its minimum (eq. 15 and 16).

$$LE_{wet} = R_n - G_0 - H_{wet} \tag{15}$$

$$H_{wet} = R_n - G_0 - LE_{wet} \tag{16}$$

The sensible heat flux at wet limit is derived from a equation similar to the Penman-Monteith equation (eq.17)

$$H_{wet} = \left(\left(R_n - G_0\right) - \frac{\rho C_p}{r_{ew}} \cdot \frac{e_{sat} - e}{\gamma} \right) \Big/ \left(1 + \frac{\Delta}{\gamma} \right) \tag{17}$$

The actual sensible heat flux (H) is given by the equation 18 and is constrained in the range set by the sensible heat flux at wet (H_{wet}) and dry (H_{dry}) limits.

$$H = \rho . C_p . \frac{\Delta t}{r_{ah}} \tag{18}$$

where, ρC_p is the volumetric heat capacity, r_{ah} is the aerodynamic resistance to heat transport and Δt is the difference between potential surface temperature and potential air temperature ($\Delta t = \theta_0 - \theta_a$).

Surface roughness parameters z_{om} and z_{oh}

Empirical relationship derived by Bastiaanssen (1998) is used to estimate the surface roughness length for momentum transfer (z_{om}) as given in equation 19.

$$Z_{om} = Exp\left(C_1 + C_2 NDVI\right) \tag{19}$$

where C_1 and C_2 are regression constants derived separately for each image from a plot of $\ln(z_{om})$ versus NDVI for pixels representing varied vegetation heights and extremes of NDVI.

A physically based model for roughness length for heat transfer (z_{oh}) is introduced in the SEBS algorithm. In this model the z_{oh} in terms of KB^{-1} ($=\ln(z_{om}/z_{oh})$) is expressed as a function of surface conditions and the aerodynamic variables. An explanation for equation 20 can be found in Su (2002).

$$kB^{-1} = \frac{kC_d}{4C_t \frac{u_*}{u(h)} \left(1 - e^{-n_{ec}/2}\right)} f_c^2 + 2 f_c \, f_s \, \frac{k \cdot {}^{u_*}\!/_{u(h)} \cdot {}^{z_{0m}}\!/_{h}}{C_t^*} + kB_s^{-1} f_s^2 \tag{20}$$

Evaluation criterion

Coefficient of determination (R^2): It describes the proportion of the variance in measured data explained by the model. R^2 ranges from 0 to 1, with higher values indicating less error variance.

$$R^2 = \frac{\left(\sum_{i=1}^{n}(O_i - \bar{O})\,(M_i - \bar{M})\right)^2}{\sum_{i=1}^{n}(O_i - \bar{O})^2 . \sum_{i=1}^{n}(M_i - \bar{M})^2} \quad (1)$$

Nash-Sutcliffe efficiency (NSE): It indicates how well the plot of observed versus simulated data fits the 1:1 line. NSE is computed as shown in equation 2. NSE ranges between $-\infty$ and 1.0 (1 inclusive), with NSE =1 being the optimal value. Values between 0.0 and 1.0 are generally viewed as acceptable levels of performance, whereas values <0.0 indicates unacceptable performance (Moriasi et. al, 2007).

$$NSE = \frac{\sum_{i=1}^{n}(O_i - \bar{O})^2 - \sum_{i=1}^{n}(M_i - O_i)^2}{\sum(O_i - \bar{O})^2} \quad (2)$$

Mean bias error (MBE) and Percent bias (PBIAS): These indicate error in the units of the constituent of interest and also as percentage error, which facilitates result analysis. A value of zero or close to zero indicates good performance of the model. The optimal value of PBIAS is 0.0, with low-magnitude values indicating accurate model simulation. Positive values indicate model underestimation bias, and negative values indicate model overestimation bias.

$$MBE = \frac{1}{n}\sum_{i=1}^{n}(M_i - O_i) \quad (3)$$

$$PBIAS = \frac{\sum_{i=1}^{n}(M_i - O_i)}{\sum O_i} * 100 \quad (4)$$

Root mean square error (RMSE) and percentage root mean square error (%RMSE): These are commonly used error index statistics with lower value range indicating better model performance.

$$RMSE = \sqrt{\frac{1}{n-1}\sum_{i=1}^{n}\{(M_i - O_i) - MBE\}^2} \quad (5)$$

$$Percent\ RMSE = \frac{RMSE}{\frac{\sum_{i=1}^{n} O_i}{n}} * 100 \quad (6)$$

where in equation 1-6, n is the number of observations points, O_i and M_i are the observed and model predicted values at each comparison point i, and $\bar{O}$ and $\bar{M}$ are the arithmetic means of the observed and modeled values.

Results and Discussion

SEBS algorithms applied on high resolution aircraft imagery showed good performance in predicting all the energy balance components (Fig.2). Net Radiation was predicted with a RMSE of 52.45 W m^{-2} (9.27%) and a MBE of 9.20 W m^{-2}

(1.63%) which was within the acceptable limits (5-10%). and close to the value reported by Chávez et al (2009). The R^2 and NSE values for R_n were 0.73 and 0.72, respectively (Fig.2b).

Table 3: SEBS estimates hourly ET evaluated at each lysimeter field and intra-day images

Lysimeter	MBE (mmh^{-1})	PBIAS (%)	RMSE (mmh^{-1})	RMSE (%)	NSE	R^2
NE	0.03	5.97	0.12	21.35	0.72	0.82
SE	0.02	3.64	0.10	9.92	0.92	.81
NW	-0.05	-10.21	0.12	22.75	0.55	0.68
SW	-0.04	-8.08	0.10	20.17	0.79	0.83
3 Intra-day image each taken at different time of the day						
7/10/07	-0.05	-8.18	0.05	8.12	0.58	0.68
7/27/07	0.03	4.61	0.09	14.21	0.72	0.77

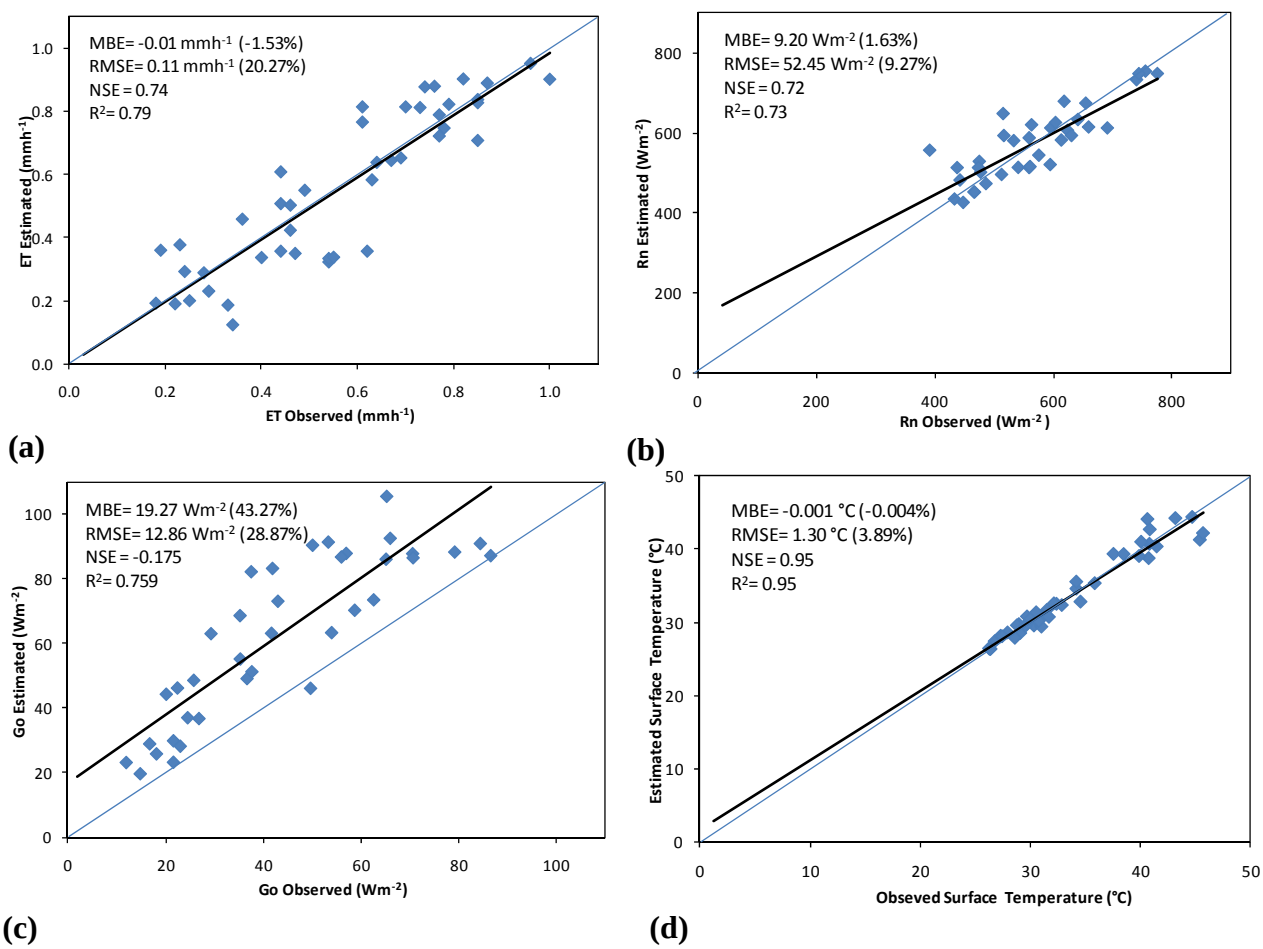

Figure 2: (a) Estimated versus observed hourly ET (b) Estimated versus observed instantaneous net radiation (c) Estimated versus observed soil heat flux (d) Estimated versus observed surface temperature.

A high positive mean bias error of 19.27 W m^{-2} (PBIAS of 43%) was seen in the evaluation of soil heat flux (G_o) indicating model over prediction. Negative NSE value (-0.175) indicated unacceptable model performance. However, high R^2 value showed linear relationship between observed and estimated values suggesting that the model has consistently over predicted the G_o values (Fig. 2c). Errors in sensor placement and instrument calibration are commonly reported with G_o measurements. Since, the magnitude of G_o is smallest in the energy balance it can be speculated that errors in its estimation will only make small difference in the overall ET estimation. Radiometric surface temperature (T_s) recorded by the thermal infrared sensor was consistent with the ground measured values and showed small error with very good fitting (Fig. 2d).

The hourly ET estimated by the SEBS algorithm showed good fitting with the observed lysimeter data (Fig.2a). Using all four lysimeter field data (44 data points), the overall error in SEBS-ET estimation was -0.01mmh^{-1} (MBE), 0.11mmh^{-1} (RMSE), -1.53% (PBIAS) and 20.27% (%RMSE). It is known that the error tends to decrease as the instantaneous ET is interpolated into daily to season values. Therefore, the error statistics in this study shows very good result for the estimated hourly ET compared to the lysimeter data. The R^2 and NSE values were 0.79 and 0.74, respectively, showing good linear relationship and model performance. With the removal of six data points (out of 44) the accuracy can be increased to 15.02% RMSE (0.08 mmd^{-1}), showing that evaluation statistics RMSE is highly sensitive to small deviations. Apart from the models limitations and measurement limitations the error can be attributed to the spatial averaging effects over the lysimeter locations. Model evaluation for each lysimeter field separately is presented in Table 2. SEBS performed equally well for the irrigated (NE and SE) and dryland (NW and SW) fields. Fitness and error analysis of the intra-day images also show good agreement with the observed ET values. Stewart et al. (1994) reported that H can be estimated accurately using radiometric surface temperature when good estimation of kB^{-1} is available. The kB^{-1} parameterization in the SEBS algorithm, involving canopy structure in terms of canopy height, LAI and fractional vegetation cover could rightly estimate the roughness length for heat transfer (z_{oh}) for the dryland and irrigated fields thus providing good ET values for the dense and sparse vegetation conditions.

Accurate radiometric surface temperature, estimation of roughness momentum transfer from canopy height measurements for each image and quality meteorological inputs, all contributed towards good estimation of hourly ET.

Summary

SEBS algorithm was applied to eleven high resolution airborne multispectral imagery acquired during early and mid cropping seasons and evaluated against lysimeter data. The hourly ET estimation error for the 44 data points was 20.3% RMSE which was close to the value (20%) reported by the developer (Su 2002). The performance of the algorithm was consistently good for irrigated (densely vegetated) and dryland (sparsely vegetated) conditions. Analysis of intra-day images showed that the diurnal variations in the fluxes were accurately captured by the algorithm.

References

Bastiaanssen, W. G. M., Menenti, M., Feddes, R. A., Holtslag, A.A.M. (1998). A remote sensing surface energy balance algorithm for land (SEBAL). 1. Formulation. Journal of Hydrology, 213:198–212

Brutsaert, W., (1975). On a derivable formula for long-wave radiation from clear skies. Water Resources Research, 11: 742-744

Chávez, J. L., Gowda, P. H., Howell, T. A., Neale, C. M. U., Copeland, K. S., (2009) Estimating hourly crop ET using a two-source energy balance model and multispectral airborne imagery. Irrigation Science, 28:79-91

Gowda, P. H., Chavez, J. L., Colaizzi, P. D., Evett, S. R., Howell, T. A., Tolk, J. A (2008). ET mapping for agricultural water management: present status and challenges. Irrigation Science, 26:223–237

Jia, L., Su, Z., Hurk, B. V. D., Menenti, M., Moene, A., Bruin, H. A. R. D. B., Yrisarry, J. J. B., Ibanez, M., Cuesta, A. (2003). Estimation of sensible heat flux using the Surface Energy Balance System (SEBS) and ATSR measurements. Physics and Chemistry of Earth, Part B: Hydrology, Ocean & Atmosphere, 28:75-88

McCabe, M. F., Wood, E. F., (2006). Scale influences on the remote estimation of evapotranspiration using multiple satellite sensors. Remote Sensing of Environment, doi:10.1016/j.rse.2006.07.006

Menenti, M. and Choudhury, B. J. (1993). Parameterization of land surface evapotranspiration using a location dependent potential evapotranspiration and surface temperature range. In: Bolle, H.J. et al. (editors), Exchange processes at the land surface for a range of space and time scale, IAHS Publ. No., 212:561-568

Menenti, M., Jia, L., Su, L. (2003). On SEBI-SEBS validation in France, Italy, Spain, USA and China. In proceedings of ICID workshop on remote sensing of ET for large regions, 17 sep 2003.

Moriasi, D. N., Arnold, J. G., Liew, M. W. V., Bingner, R. L., Harmel, R. D., Veith, T. L., (2007). Model evaluation guidelines for systematic quatification of accuracy in watershed simulations. Transactions of ASABE, 50(3): 885-900

Stewart, J. B., Kustas, W. P., Humes, K. S., Nichols, W. D., Moran, M. S., De Bruin, H. A. R., (1994). Sensible heat flux - radiometric surface temperature relationship for eight semi arid areas. Journal of Applied Meteorology, 33:1110-1117.

Su, Z., Timmermans, W., Gieske, A., et al. (2008). Quantification of land–atmosphere exchanges of water, energy and carbon dioxide in space and time over the heterogeneous Barrax site. International Journal of Remote Sensing, 29:5215-5235

Su, Z. (2002). The Surface Energy Balance System (SEBS) for estimation of turbulent heat fluxes. Hydrology and Earth System Sciences, 6:85-99

Van der Kwast, J., Timmermans, W., Gieske, A., Su, Z., Olioso, A., Jia, L., Elbers, J., Karssenberg, D., de Jong, S., (2009). Evaluation of the Surface Energy Balance System (SEBS) applied to ASTER imagery with flux-measurements at the SPARC 2004 site (Barrax, Spain). Hydrology and Earth System Sciences, 13:1337-1347